PHYSICAL REVIEW D **80,** 014025 (2009)

Scalar, axial-vector, and tensor resonances from the ρD^*, ωD^* interaction in the hidden gauge formalism

R. Molina,[1] H. Nagahiro,[2,3] A. Hosaka,[3] and E. Oset[1]

[1]*Departamento de Física Teórica and IFIC, Centro Mixto Universidad de Valencia-CSIC, Institutos de Investigación de Paterna, Apartado 22085, 46071 Valencia, Spain*

[2]*Department of Physics, Nara Women's University, Nara 630-8506, Japan*

[3]*Research Center for Nuclear Physics (RCNP), Osaka University, Ibaraki, Osaka 567-0047, Japan*

(Received 23 March 2009; published 29 July 2009)

We study composite systems of light (ρ and ω) and heavy (D^*) vector mesons by using the interaction within the hidden gauge formalism. We find a strong attraction in the isospin, spin channels $(I, S) = (1/2, 0)$, $(1/2, 1)$, and $(1/2, 2)$ with positive parity. The attraction is large enough to strongly bind these mesons in states with these quantum numbers, leading to states which can be identified with $D_2^*(2460)$ and probably with $D^*(2640)$, the last one without experimental spin and parity assignment. In the case of $I = 3/2$, one obtains repulsion and thus, no exotic mesons in this sector are generated in the approach.

DOI: 10.1103/PhysRevD.80.014025 PACS numbers: 13.75.Lb, 12.40.Vv, 12.40.Yx, 14.40.Cs

I. INTRODUCTION

Recently a study of the $\rho\rho$ interaction with the hidden gauge formalism [1–3] was carried out in [3]. The hidden gauge symmetry (HGS) was introduced by Bando, Kugo, and Yamawaki where the ρ meson was regarded as a dynamical gauge boson of the HGS of the nonlinear sigma model. One interesting fact which is relevant in this discussion is that there is a strong attraction in the isospin and spin channels $(I, S) = (0, 0)$ and (0,2), which is enough to bind the $\rho\rho$ system leading to a tensor and a scalar meson which could be identified with the $f_0(1370)$ and $f_2(1270)$ meson states [4]. In a later work the radiative decay of these states in $\gamma\gamma$, a channel with rates very sensitive to the nature of the resonances, was studied [5] obtaining results in agreement with the PDG [6] for the case of the tensor state and in qualitative agreement with preliminary results at Belle for the scalar state [7]. The work of [3] has been recently extended to SU(3) for the interaction of the vectors of the nonet, where several states, which can be identified with existing resonances, are also dynamically generated [8]. The success of the approach encourages us to study the charm sector in the lightest case, the one for the interaction of the ρ, ω, and D^* mesons. Another possible approach to this work could be done following the lines of [9] for a meson-baryon interaction involving SU(8) symmetry. Work in this direction is in progress [10], but we can advance that, while for pseudoscalar-baryon interaction the approaches are equivalent. When vector mesons are involved the results are very different [11].

The starting point in our approach is the interaction of vector mesons among themselves provided by the hidden gauge formalism, which now has to be generalized to SU(4) to accommodate the charm vectors D^* into the framework. Admitting that SU(4) is more strongly broken than SU(3), the SU(4) symmetry is invoked in the basic hidden gauge Lagrangians, but is already broken in the vector exchange diagrams that provide the amplitudes for the vector-vector interaction. What we find is a strong attraction in the isospin, spin channels $(I, S) = (1/2, 0)$, $(1/2, 1)$, and $(1/2, 2)$, which leads to bound $\rho(\omega)D^*$ states in all these channels. In the case of $I = 3/2$, we find repulsion and hence we do not generate states that would qualify as exotic from the $q\bar{q}$ picture. The states that we find qualify as mostly ρD^* molecules and fit nicely with the experimental states $D_2^*(2460)$ and $D^*(2640)$. The present study would, thus, suggest for these states a different nature than the one usually assumed in terms of $q\bar{q}$ states [6,12,13].

II. FORMALISM FOR *VV* INTERACTION

A. Lagrangian

We follow the formalism of the HGS for vector mesons of [1,2] (see also [14] for a practical set of Feynman rules). The Lagrangian involving the interaction of vector mesons among themselves is given by

$$\mathcal{L}_{III} = -\tfrac{1}{4}\langle V_{\mu\nu} V^{\mu\nu}\rangle, \tag{1}$$

where the symbol $\langle\,\rangle$ stands for the trace in the SU(4) space and $V_{\mu\nu}$ is given by

$$V_{\mu\nu} = \partial_\mu V_\nu - \partial_\nu V_\mu - ig[V_\mu, V_\nu], \tag{2}$$

with g given by

$$g = \frac{M_V}{2f}, \tag{3}$$

and $f = 93$ MeV as the pion decay constant. The value of g of Eq. (3) is one of the ways to account for the Kawarabayashi-Suzuki-Fayyazuddin-Riazuddin (KSFR) relation [15] which is tied to vector meson dominance [16]. The vector field V_μ is represented by the SU(4) matrix which is parametrized by 16 vector mesons includ-

ing 15-plet and a singlet of SU(4),

$$V_\mu = \begin{pmatrix} \frac{\rho^0}{\sqrt{2}} + \frac{\omega}{\sqrt{2}} & \rho^+ & K^{*+} & \bar{D}^{*0} \\ \rho^- & -\frac{\rho^0}{\sqrt{2}} + \frac{\omega}{\sqrt{2}} & K^{*0} & D^{*-} \\ K^{*-} & \bar{K}^{*0} & \phi & D_s^{*-} \\ D^{*0} & D^{*+} & D_s^{*+} & J/\psi \end{pmatrix}_\mu , \quad (4)$$

where the ideal mixing has been taken for ω, ϕ, and J/ψ. The interaction of $\mathcal{L}_{III}$ gives rise to a contact term coming for $[V_\mu, V_\nu][V_\mu, V_\nu]$

$$\mathcal{L}_{III}^{(c)} = \frac{g^2}{2}\langle V_\mu V_\nu V^\mu V^\nu - V_\nu V_\mu V^\mu V^\nu \rangle, \quad (5)$$

depicted in Fig. 1(a), and, on the other hand, it gives rise to a three-vector vertex

$$\mathcal{L}_{III}^{(3V)} = ig\langle (\partial_\mu V_\nu - \partial_\nu V_\mu) V^\mu V^\nu \rangle, \quad (6)$$

depicted in Fig. 1(b). This latter Lagrangian gives rise to a $VV \to VV$ interaction by means of the exchange of one of the vectors, as shown in Fig. 1(c).

The SU(4) structure of the Lagrangian allows us to take into account all the channels within SU(4) which couple to certain quantum numbers. In this work we shall present results for the case of the ρD^* interaction. The formalism is the same as that used in [4]. Some approximations were made there which make the formalism handy and reliable, by neglecting the three-momentum of the vector mesons with respect to their masses. It is interesting to see that with this approximation one obtains [14] from the hidden gauge approach, the chiral local Lagrangians which are used to study the interaction of pseudoscalar mesons among themselves and the pseudoscalar mesons with vector mesons and with baryons [17,18].

B. Four-vector contact interaction

Starting with the Lagrangian of Eq. (5) we can immediately obtain the amplitude of, for instance, $\rho^+ D^{*0} \to \rho^+ D^{*0}$ corresponding to Fig. 2, in the particle base,

$$\begin{aligned} -it^{(c)}_{\rho^+ D^{*0} \to \rho^+ D^{*0}} = ig^2 (& 2\epsilon^{(1)}_\mu \epsilon^{(2)}_\nu \epsilon^{(3)\nu} \epsilon^{(4)\mu} \\ & - \epsilon^{(1)}_\mu \epsilon^{(2)}_\mu \epsilon^{(3)\nu} \epsilon^{(4)\nu} \\ & - \epsilon^{(1)}_\nu \epsilon^{(2)}_\mu \epsilon^{(3)\nu} \epsilon^{(4)\mu}), \end{aligned} \quad (7)$$

where the indices 1, 2, 3, and 4 correspond to the particles

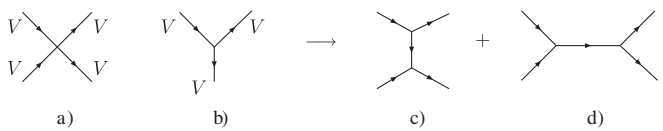

FIG. 1. Terms of the $\mathcal{L}_{III}$ Lagrangian: (a) four-vector contact term, Eq. (5); (b) three-vector interaction, Eq. (6); (c) t and u channels from vector exchange; and (d) s channel for vector exchange.

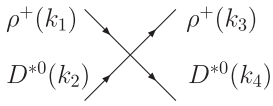

FIG. 2. Contact term of the $\rho\rho$ interaction.

with momenta k_1, k_2, k_3, and k_4 in Fig. 2. It is straightforward to write down all amplitudes for other channels.

In the approximation of neglecting the three-momenta of the vector mesons, only the spatial components of the polarization vectors are nonvanishing and then one can easily obtain spin projection operators [4] into spin 0, 1, 2 states, which are given here:

$$\begin{aligned} \mathcal{P}^{(0)} &= \tfrac{1}{3}\epsilon_\mu \epsilon^\mu \epsilon_\nu \epsilon^\nu, \\ \mathcal{P}^{(1)} &= \tfrac{1}{2}(\epsilon_\mu \epsilon_\nu \epsilon^\mu \epsilon^\nu - \epsilon_\mu \epsilon_\nu \epsilon^\nu \epsilon^\mu), \\ \mathcal{P}^{(2)} &= \{\tfrac{1}{2}(\epsilon_\mu \epsilon_\nu \epsilon^\mu \epsilon^\nu + \epsilon_\mu \epsilon_\nu \epsilon^\nu \epsilon^\mu) - \tfrac{1}{3}\epsilon_\mu \epsilon^\mu \epsilon_\nu \epsilon^\nu\}, \end{aligned} \quad (8)$$

where the order 1, 2, 3, 4 in the polarization vectors is understood. We can then write the combination of polarization vectors appearing in Eq. (7) in terms of the spin combinations and thus we obtain the kernel of the interaction which will be used later to solve the Bethe-Salpeter equation. However, it is practical to construct the isospin combinations before the spin projection is done.

Recalling that we have an isospin doublet with $(-D^{*0}, D^{*+})$ and one isospin triplet, $(\rho^-, \rho^0, -\rho^+)$, the $I = 1/2$ and $3/2$ combinations are written as

$$\begin{aligned} |\rho D^*, I = 1/2, I_3 = 1/2\rangle &= \sqrt{\frac{2}{3}}|\rho^+ D^{*0}\rangle - \frac{1}{\sqrt{3}}|\rho^0 D^{*+}\rangle, \\ |\rho D^*, I = 1/2, I_3 = 3/2\rangle &= \frac{1}{\sqrt{3}}|\rho^+ D^{*0}\rangle + \sqrt{\frac{2}{3}}|\rho^0 D^{*+}\rangle. \end{aligned} \quad (9)$$

We then find the amplitudes in the isospin base by forming linear combinations of the amplitudes in the particle base weighted by the Clebsh-Gordan coefficients as given in Eq. (9),

$$\begin{aligned} t^{(I=1/2)} &= g^2(-\tfrac{7}{2}\epsilon_\mu \epsilon_\nu \epsilon^\nu \epsilon^\mu + \tfrac{5}{2}\epsilon_\mu \epsilon^\mu \epsilon_\nu \epsilon^\nu + \epsilon_\mu \epsilon_\nu \epsilon^\mu \epsilon^\nu), \\ t^{(I=3/2)} &= g^2(\epsilon_\mu \epsilon_\nu \epsilon^\nu \epsilon^\mu + \epsilon_\mu \epsilon_\nu \epsilon^\mu \epsilon^\nu - 2\epsilon_\mu \epsilon^\mu \epsilon_\nu \epsilon^\nu). \end{aligned} \quad (10)$$

These amplitudes, after projection into the spin channels, give rise to the following kernels (potential) for $I = 1/2$:

$$\begin{aligned} t^{(I=1/2,S=0)} = +5g^2, \qquad t^{(I=1/2,S=1)} = +\tfrac{9}{2}g^2, \\ t^{(I=1/2,S=2)} = -\tfrac{5}{2}g^2, \end{aligned} \quad (11)$$

and also for the case of $I = 3/2$,

$$\begin{aligned} t^{(I=3/2,S=0)} = -4g^2, \qquad t^{(I=3/2,S=1)} = 0, \\ t^{(I=3/2,S=2)} = +2g^2. \end{aligned} \quad (12)$$

When one or two ρ meson(s) are replaced by the ω meson(s), where there is only one isospin state $I = 1/2$, we

find the following interaction terms:

$$t^{(I=1/2)}_{\rho D^*\to\omega D^*} = \frac{\sqrt{3}}{2} g^2 (2\epsilon_\mu \epsilon_\nu \epsilon^\mu \epsilon^\nu - \epsilon_\mu \epsilon_\nu \epsilon^\nu \epsilon^\mu - \epsilon_\mu \epsilon^\mu \epsilon_\nu \epsilon^\nu),$$
$$t^{(I=1/2)}_{\omega D^*\to\omega D^*} = -\frac{1}{2} g^2 (\epsilon_\mu \epsilon_\nu \epsilon^\nu \epsilon^\mu + \epsilon_\mu \epsilon^\mu \epsilon_\nu \epsilon^\nu - 2\epsilon_\mu \epsilon_\nu \epsilon^\mu \epsilon^\nu). \quad (13)$$

After projection in spin they become for $\rho D^* \to \omega D^*$,

$$t^{(I=1/2,S=0)}_{\rho D^*\to\omega D^*} = -\sqrt{3} g^2, \qquad t^{(I=1/2,S=1)}_{\rho D^*\to\omega D^*} = +\frac{3\sqrt{3}}{2} g^2,$$
$$t^{(I=1/2,S=2)}_{\rho D^*\to\omega D^*} = +\frac{\sqrt{3}}{2} g^2, \quad (14)$$

and in the same way, we have for $\omega D^* \to \omega D^*$,

$$t^{(I=1/2,S=0)}_{\omega D^*\to\omega D^*} = -g^2, \qquad t^{(I=1/2,S=1)}_{\omega D^*\to\omega D^*} = +\tfrac{3}{2} g^2,$$
$$t^{(I=1/2,S=2)}_{\omega D^*\to\omega D^*} = +\tfrac{1}{2} g^2. \quad (15)$$

C. ρ meson exchange terms

From the Lagrangian of Eq. (6) we get the three-vector vertex as depicted in Fig. 3. For practical purposes it is convenient to rewrite the three-vector Lagrangian of Eq. (6) as

$$\mathcal{L}^{(3V)}_{III} = ig\langle V^\nu \partial_\mu V_\nu V^\mu - \partial_\nu V_\mu V^\mu V^\nu \rangle = ig\langle (V^\mu \partial_\nu V_\mu - \partial_\nu V_\mu V^\mu) V^\nu \rangle. \quad (16)$$

In Eq. (16) we have a three-vector vertex, where any of the three-vector fields can correspond in principle to the exchanged vector in the diagram of Fig. 1(c). Nevertheless, by assuming that the three-momenta of the external vectors can be neglected as compared with the vector mass, the polarization vectors of the external vector mesons have only spatial components. Then by looking at the Lagrangian of Eq. (16) we see that the field V^ν cannot correspond to an external vector meson. Indeed, if this were the case, the ν index must be spatial and then the partial derivative ∂_ν is replaced by a three-momentum of the vector mesons which is neglected in the approach. Then V^ν corresponds to the exchanged vector and this simplifies the calculation. The approximation of neglecting the three-momenta of the external vectors corresponds to the consideration of only the s wave.

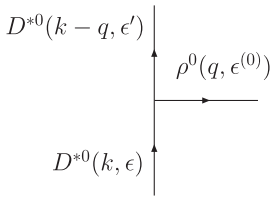

FIG. 3. Three-vector vertex diagram.

The vertex function corresponding to the diagram of Fig. 3 is given by

$$-it^{(3)} = -\frac{g}{\sqrt{2}} \{ (iq_\mu \epsilon^{(0)}_\nu - iq_\nu \epsilon^{(0)}_\mu) \epsilon'^\mu \epsilon^\nu + (i(k-q)_\mu \epsilon'_\nu - i(k-q)_\nu \epsilon'_\mu) \epsilon^\mu \epsilon^{(0)\nu} + (-ik_\mu \epsilon_\nu + ik_\nu \epsilon_\mu) \epsilon^{(0)\mu} \epsilon'^\nu \}. \quad (17)$$

With this basic structure we can readily evaluate the amplitude of the first diagram of Fig. 4 to obtain

$$-it^{(\mathrm{ex})}_{\rho^+ D^{*0}\to\rho^+ D^{*0}} = -\sqrt{2} g \{ (-i(k_3-k_1)_\mu \epsilon^{(0)}_\nu + i(k_3-k_1)_\nu \epsilon^{(0)}_\mu) \epsilon^{(1)\mu} \epsilon^{(3)\nu} + (-ik_{1\mu} \epsilon^{(1)}_\nu + ik_{1\nu} \epsilon^{(1)}_\mu) \epsilon^{(3)\mu} \epsilon^{(0)\nu} + (ik_{3\mu} \epsilon^{(3)}_\nu - ik_{3\nu} \epsilon^{(3)}_\mu) \epsilon^{(0)\mu} \epsilon^{(1)\nu} \} \frac{i}{(k_3-k_1)^2 - M_\rho^2 + i\epsilon} - \frac{g}{\sqrt{2}} \{ (i(k_2-k_4)_\mu \epsilon^{(0)}_\nu - i(k_2-k_4)_\nu \epsilon^{(0)}_\mu) \epsilon^{(4)\mu} \epsilon^{(2)\nu} + (ik_{4\mu} \epsilon^{(4)}_\nu - ik_{4\nu} \epsilon^{(4)}_\mu) \epsilon^{(2)\mu} \epsilon^{(0)\nu} + (-ik_{2\mu} \epsilon^{(2)}_\nu + ik_{2\nu} \epsilon^{(2)}_\mu) \epsilon^{(0)\mu} \epsilon^{(4)\nu} \}. \quad (18)$$

Recalling that the three-momenta of the external particles is small and neglected, we arrive at the following expression:

$$t^{(\mathrm{ex})}_{\rho^+ D^{*0}\to\rho^+ D^{*0}} = -\frac{g^2}{M_\rho^2} (k_1+k_3)\cdot(k_2+k_4) \epsilon_\mu \epsilon_\nu \epsilon^\mu \epsilon^\nu. \quad (19)$$

By looking at the structure of the second diagram in Fig. 4 we find the following result for the amplitude:

$$t^{(\mathrm{ex})}_{\rho^+ D^{*0}\to\rho^0 D^{*+}} = \sqrt{2} \frac{g^2}{M_\rho^2} (k_1+k_3)\cdot(k_2+k_4) \epsilon_\mu \epsilon_\nu \epsilon^\mu \epsilon^\nu. \quad (20)$$

We note that the amplitude $\rho^0 D^* \to \rho^0 D^*$ with ρ^0 ex-

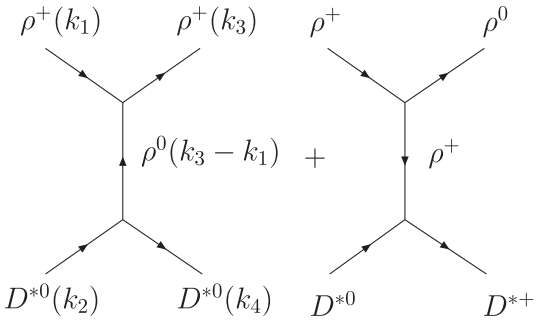

FIG. 4. Vector exchange diagrams for $\rho D^* \to \rho D^*$.

change vanishes because the three-ρ^0 vertex does not exist due to isospin invariance. We can see that in all the cases the combination of vector polarizations is the same. The isospin projections give us

$$t^{(\mathrm{ex},I=1/2)}_{\rho D^*\to\rho D^*} = -2\frac{g^2}{M_\rho^2}(k_1+k_3)\cdot(k_2+k_4)\epsilon_\mu\epsilon_\nu\epsilon^\mu\epsilon^\nu,$$
$$t^{(\mathrm{ex},I=3/2)}_{\rho D^*\to\rho D^*} = \frac{g^2}{M_\rho^2}(k_1+k_3)\cdot(k_2+k_4)\epsilon_\mu\epsilon_\nu\epsilon^\mu\epsilon^\nu. \tag{21}$$

Now using the equations for the spin projections we can split the terms into their spin parts and we obtain

$$t^{(\mathrm{ex},I=1/2,S=0,1,2)}_{\rho D^*\to\rho D^*} = -2\frac{g^2}{M_\rho^2}(k_1+k_3)\cdot(k_2+k_4),$$
$$t^{(\mathrm{ex},I=3/2,S=0,1,2)}_{\rho D^*\to\rho D^*} = \frac{g^2}{M_\rho^2}(k_1+k_3)\cdot(k_2+k_4), \tag{22}$$

that is, we find spin degeneration in the amplitudes which involve the exchange of one ρ meson. These structures can be simplified using momentum conservation and one finds

$$t^{(\mathrm{ex},I=1/2,S=0,1,2)}_{\rho D^*\to\rho D^*} = -2\frac{g^2}{M_\rho^2}\left\{\frac{3}{2}s - m_\rho^2 - m_{D^*}^2 - \frac{(m_\rho^2-m_{D^*}^2)^2}{2s}\right\},$$
$$t^{(\mathrm{ex},I=3/2,S=0,1,2)}_{\rho D^*\to\rho D^*} = +\frac{g^2}{M_\rho^2}\left\{\frac{3}{2}s - m_\rho^2 - m_{D^*}^2 - \frac{(m_\rho^2-m_{D^*}^2)^2}{2s}\right\}. \tag{23}$$

The expressions of Eq. (23) correspond to on-shell vectors in the sense that their four-momenta are required to fulfill $q^2 = M_V^2$, which allows one to write the expressions of Eq. (22) in terms of the variable s, upon projection on s wave and neglecting the three-momenta of the particles. In the above equations (19)–(23), we have also neglected the exchanged momentum and replaced the ρ-meson propagator by $1/M_\rho^2$. This is obvious if in the two momenta k_1 and k_3 of Fig. 4, the spatial part is considered small.

Note that for the exchange of a vector we do not have a contribution from the ωD^* channel. Indeed, the vertex $\omega\omega\omega$ and $\rho\rho\omega$ violate G parity, and the $\rho\omega\omega$ violates isospin. In the next section we consider the amplitudes which include also the exchange of one heavy vector meson, but we anticipate that the amplitudes calculated so far are more relevant than the other ones.

D. D^*-exchange terms

In this section we are going to take into account the exchange of one heavy vector meson, D^* or $\bar{D}^*$, in the channels ρD^* and ωD^*, by means of the diagrams in Fig. 5. Note that in Fig. 5 the vertex $\omega\omega D^*$ does not appear because it violates isospin. By means of the Lagrangian of Eq. (6) we arrive at the following amplitudes for the first and second diagrams depicted in that figure:

$$t^{(D^*-\mathrm{ex})}_{\rho^+D^{*0}\to\rho^0D^{*+}} = \frac{1}{\sqrt{2}}\frac{g^2}{M_{D^*}^2}(k_1+k_4)\cdot(k_2+k_3)\epsilon_\mu\epsilon_\nu\epsilon^\nu\epsilon^\mu,$$
$$t^{(D^*-\mathrm{ex})}_{\rho^0D^{*+}\to\rho^0D^{*+}} = \frac{1}{2}\frac{g^2}{M_{D^*}^2}(k_1+k_4)\cdot(k_2+k_3)\epsilon_\mu\epsilon_\nu\epsilon^\nu\epsilon^\mu. \tag{24}$$

The isospin decomposition can be done as before by making weighted sums of Eq. (24). We find

$$t^{(D^*-\mathrm{ex},I=1/2)}_{\rho D^*\to\rho D^*} = -\frac{1}{2}\frac{\kappa g^2}{M_\rho^2}(k_1+k_4)\cdot(k_2+k_3)\epsilon_\mu\epsilon_\nu\epsilon^\nu\epsilon^\mu,$$
$$t^{(D^*-\mathrm{ex},I=3/2)}_{\rho D^*\to\rho D^*} = \frac{\kappa g^2}{M_\rho^2}(k_1+k_4)\cdot(k_2+k_3)\epsilon_\mu\epsilon_\nu\epsilon^\nu\epsilon^\mu, \tag{25}$$

where $\kappa = M_\rho^2/M_{D^*}^2$. Upon spin projection we find

$$t^{(D^*-\mathrm{ex},I=1/2,S=0,2)}_{\rho D^*\to\rho D^*} = -\frac{1}{2}\frac{\kappa g^2}{M_\rho^2}(k_1+k_4)\cdot(k_2+k_3),$$
$$t^{(D^*-\mathrm{ex},I=1/2,S=1)}_{\rho D^*\to\rho D^*} = \frac{1}{2}\frac{\kappa g^2}{M_\rho^2}(k_1+k_4)\cdot(k_2+k_3), \tag{26}$$

and similarly for $I = 3/2$,

$$t^{(D^*-\mathrm{ex},I=3/2,S=0,2)}_{\rho D^*\to\rho D^*} = \frac{\kappa g^2}{M_\rho^2}(k_1+k_4)\cdot(k_2+k_3),$$
$$t^{(D^*-\mathrm{ex},I=3/2,S=1)}_{\rho D^*\to\rho D^*} = -\frac{\kappa g^2}{M_\rho^2}(k_1+k_4)\cdot(k_2+k_3). \tag{27}$$

Again by neglecting the three-momenta of the external

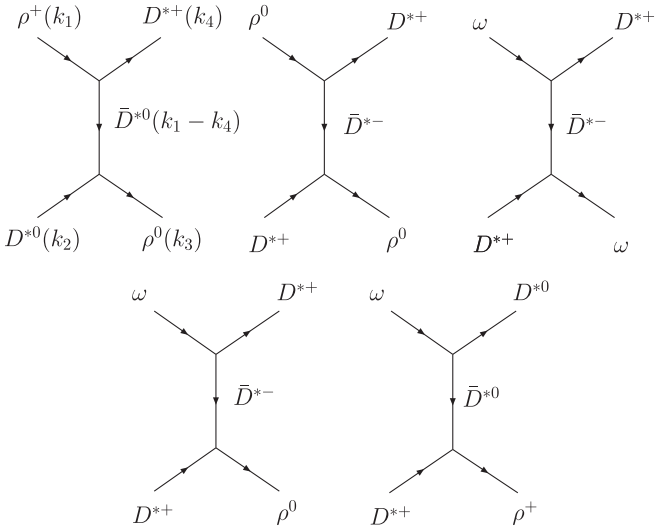

FIG. 5. Diagrams including the exchange of one heavy vector meson.

particles and by taking the center-of-mass reference system, one can express the factors which involve momenta as

$$(k_1+k_3)\cdot(k_2+k_4)=\frac{3}{2}s-m_\rho^2-m_{D^*}^2-\frac{(m_\rho^2-m_{D^*}^2)^2}{2s},$$
$$(k_1+k_4)\cdot(k_2+k_3)=\frac{3}{2}s-m_\rho^2-m_{D^*}^2+\frac{(m_\rho^2-m_{D^*}^2)^2}{2s}. \quad (28)$$

As we can observe, the spin degeneracy seen in the ρ-meson exchange amplitudes is lost in the D^*-exchange amplitudes. However, it is broken only a little due to the suppressing factor $\kappa=m_\rho^2/m_{D^*}^2\sim 0.15$.

The results are summarized in the columns titled D^* exchange in Tables I, II, and III. These new terms represent corrections of the order of 10% of the ρ-exchange ones. As can be observed in the total amplitudes, we find an attraction in the sector $I=1/2$, whereas the sector $I=3/2$ turns out repulsive. It is interesting to see that the exotic $I=3/2$ channel has a repulsive interaction. This seems to be rather universal in these kinds of studies [8,19,20].

E. T matrix

The results obtained in Tables I, II, and III provide the kernel or potential V to be used in the Bethe-Salpeter equation in its on-shell factorized form,

$$T=\frac{V}{1-VG}, \quad (29)$$

for each spin-isospin channel independently. Here G is the two meson loop function

$$G=i\int\frac{d^4q}{(2\pi)^4}\frac{1}{q^2-m_1^2+i\epsilon}\frac{1}{(P-q)^2-m_2^2+i\epsilon}, \quad (30)$$

which upon using dimensional regularization can be recast as

$$G=\frac{1}{16\pi^2}\left(\alpha+\log\frac{m_1^2}{\mu^2}+\frac{m_2^2-m_1^2+s}{2s}\log\frac{m_2^2}{m_1^2}+\frac{p}{\sqrt{s}}\left(\log\frac{s-m_2^2+m_1^2+2p\sqrt{s}}{-s+m_2^2-m_1^2+2p\sqrt{s}}+\log\frac{s+m_2^2-m_1^2+2p\sqrt{s}}{-s-m_2^2+m_1^2+2p\sqrt{s}}\right)\right), \quad (31)$$

where P is the total four-momentum of the two mesons, and p is the three-momentum of the mesons in the center-of-mass frame. Analogously, using a cutoff one obtains

$$G=\int_0^{q_{\max}}\frac{q^2dq}{(2\pi)^2}\frac{\omega_1+\omega_2}{\omega_1\omega_2[(P^0)^2-(\omega_1+\omega_2)^2+i\epsilon]}, \quad (32)$$

where $q_{\max}$ stands for the cutoff, $\omega_i=(\vec{q}_i^{\,2}+m_i^2)^{1/2}$, and the center-of-mass energy $(P^0)^2=s$.

It should be noted that the on-shell factorization, in which V of Eq. (29) is taken on shell, which means taking $q^2=M_V^2$ for the external vector lines in $VV\to VV$, is based on the N/D method of unitarization with chiral Lagrangians of [21,22]. This means that in the terms VGV of the loop expansion of Eq. (29), the kernel V accounting for the diagrams for ρ exchange must be evaluated as a function of s as if all the four vector lines different from the exchanged vector meson were like ex-

TABLE I. $V(\rho D^*\to\rho D^*)$ for the different spin-isospin channels including the exchange of one heavy vector meson. The approximate total is obtained at the threshold of ρD^*.

I	S	Contact	ρ exchange	D^* exchange	$\sim$Total $[I(J^P)]$
1/2	0	$+5g^2$	$-2\frac{g^2}{M_\rho^2}(k_1+k_3)\cdot(k_2+k_4)$	$-\frac{1}{2}\frac{\kappa g^2}{M_\rho^2}(k_1+k_4)\cdot(k_2+k_3)$	$-16g^2[1/2(0^+)]$
1/2	1	$+\frac{9}{2}g^2$	$-2\frac{g^2}{M_\rho^2}(k_1+k_3)\cdot(k_2+k_4)$	$+\frac{1}{2}\frac{\kappa g^2}{M_\rho^2}(k_1+k_4)\cdot(k_2+k_3)$	$-14.5g^2[1/2(1^+)]$
1/2	2	$-\frac{5}{2}g^2$	$-2\frac{g^2}{M_\rho^2}(k_1+k_3)\cdot(k_2+k_4)$	$-\frac{1}{2}\frac{\kappa g^2}{M_\rho^2}(k_1+k_4)\cdot(k_2+k_3)$	$-23.5g^2[1/2(2^+)]$
3/2	0	$-4g^2$	$+\frac{g^2}{M_\rho^2}(k_1+k_3)\cdot(k_2+k_4)$	$+\frac{\kappa g^2}{M_\rho^2}(k_1+k_4)\cdot(k_2+k_3)$	$+8g^2[3/2(0^+)]$
3/2	1	0	$+\frac{g^2}{M_\rho^2}(k_1+k_3)\cdot(k_2+k_4)$	$-\frac{\kappa g^2}{M_\rho^2}(k_1+k_4)\cdot(k_2+k_3)$	$+8g^2[3/2(1^+)]$
3/2	2	$+2g^2$	$+\frac{g^2}{M_\rho^2}(k_1+k_3)\cdot(k_2+k_4)$	$+\frac{\kappa g^2}{M_\rho^2}(k_1+k_4)\cdot(k_2+k_3)$	$+14g^2[3/2(2^+)]$

TABLE II. $V(\rho D^*\to\omega D^*)$ for the different spin-isospin channels including the exchange of one heavy vector meson. The approximate total is obtained at the threshold of ρD^*.

I	S	Contact	ρ exchange	D^* exchange	$\sim$Total $[I(J^P)]$
1/2	0	$-\sqrt{3}g^2$	$\cdots$	$+\frac{\sqrt{3}}{2}\frac{\kappa g^2}{M_\rho^2}(k_1+k_4)\cdot(k_2+k_3)$	$0[1/2(0^+)]$
1/2	1	$+\frac{3\sqrt{3}}{2}g^2$	$\cdots$	$-\frac{\sqrt{3}}{2}\frac{\kappa g^2}{M_\rho^2}(k_1+k_4)\cdot(k_2+k_3)$	$\frac{\sqrt{3}}{2}g^2[1/2(1^+)]$
1/2	2	$+\frac{\sqrt{3}}{2}g^2$	$\cdots$	$+\frac{\sqrt{3}}{2}\frac{\kappa g^2}{M_\rho^2}(k_1+k_4)\cdot(k_2+k_3)$	$\frac{3\sqrt{3}}{2}g^2[1/2(2^+)]$

TABLE III. $V(\omega D^* \to \omega D^*)$ for the different spin-isospin channels including the exchange of one heavy vector meson. The approximate total is obtained at the threshold of ρD^*.

I	S	Contact	ρ exchange	D^* exchange	$\sim$Total $[I(J^P)]$
1/2	0	$-g^2$	$\cdots$	$+\frac{1}{2}\frac{\kappa g^2}{M_\rho^2}(k_1+k_4)\cdot(k_2+k_3)$	$0[1/2(0^+)]$
1/2	1	$+\frac{3}{2}g^2$	$\cdots$	$-\frac{1}{2}\frac{\kappa g^2}{M_\rho^2}(k_1+k_4)\cdot(k_2+k_3)$	$\frac{1}{2}g^2[1/2(1^+)]$
1/2	2	$+\frac{1}{2}g^2$	$\cdots$	$+\frac{1}{2}\frac{\kappa g^2}{M_\rho^2}(k_1+k_4)\cdot(k_2+k_3)$	$\frac{3}{2}g^2[1/2(2^+)]$

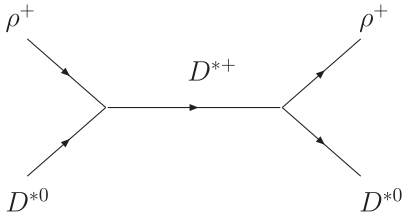

FIG. 6. S-channel D^* exchange diagram.

ternal lines. In such a case one can see that neglecting q^2/M_V^2 in the propagators, as done in our approach, is a good approximation. However, in the loop functions, Eq. (30), the propagators must be taken with their full off-shell structure to perform the integrals [21,22].

The on-shell factorization appears when the contribution of the left-hand cut is neglected in a dispersion relation of the N/D method. However, this contribution is small and smoothly energy dependent such that it can be incorporated in terms of the substraction constant in the region of interest to us.

Equation (29) in $I = 1/2$ is a 2×2 matrix equation with the amplitudes $\rho D \to \rho D$, $\rho D \to \omega D$, and $\omega D \to \omega D$ in the elements (1,1), (1,2), and (2,2).

The formalism that we are using is also allowed for s-channel ρ or D exchange and we can have the diagram of Fig. 6. But we found in [4] that this leads to a p-wave interaction for equal masses of the vectors, and only to a minor component of s wave in the case of different masses [8].

III. CONVOLUTION DUE TO THE ρ MASS DISTRIBUTION

The strong attraction in the $I = 1/2$ and $S = 0$, 1, 2 channels will produce ρD^* bound states with no width within the present treatment so far. However, this is not strictly true because the ρ meson has a large width or equivalently a mass distribution that allows the states obtained to decay in ρD^* for the low mass components of the ρ mass distribution. To take this into account we follow the traditional method which is to convolute the G function for the mass distribution of the ρ meson [14] replacing the G function by $\tilde{G}$ as follows:

$$\tilde{G}(s) = \frac{1}{N}\int_{(m_\rho-2\Gamma_\rho)^2}^{(m_\rho+2\Gamma_\rho)^2} d\tilde{m}_1^2\left(-\frac{1}{\pi}\right) Im\frac{1}{\tilde{m}_1^2 - m_\rho^2 + i\Gamma\tilde{m}_1} \times G(s,\tilde{m}_1^2, m_{D^*}^2), \quad (33)$$

with

$$N = \int_{(m_\rho-2\Gamma_\rho)^2}^{(m_\rho+2\Gamma_\rho)^2} d\tilde{m}_1^2\left(-\frac{1}{\pi}\right) Im\frac{1}{\tilde{m}_1^2 - m_\rho^2 + i\Gamma\tilde{m}_1}, \quad (34)$$

where $\Gamma_\rho = 146.2$ MeV, and for $\Gamma \equiv \Gamma(\tilde{m})$ we take the ρ width for the decay into the pions in p wave

$$\Gamma(\tilde{m}) = \Gamma_\rho\left(\frac{\tilde{m}^2 - 4m_\pi^2}{m_\rho^2 - 4m_\pi^2}\right)^{3/2}\theta(\tilde{m} - 2m_\pi). \quad (35)$$

The use of $\tilde{G}$ in Eq. (29) provides a width to the states obtained as we will see in the next section.

IV. RESULTS

When one introduces the amplitudes obtained in Tables I, II, and III as a kernel V in Eq. (29), one finds bound states with zero width in the three different cases $I = 1/2$ and $S = 0$, 1, and 2. The pole positions are given in Table IV. In Eq. (31) we have fixed the value of μ as 1500 MeV and we have fine-tuned the subtraction constant, α, around its natural value of -2 [22] in order to get the position of the $S = 2$ resonance at its value of the PDG. To quantify the freedom one has in this fine-tuning we quote that the value of the mass that we obtain using $\alpha = -2$ is 2346 MeV. The value of α for the pole positions given in Table IV is -1.74.

As was explained in the previous section, the loop function G must be convoluted to take into account the width of the ρ meson. When we do it, we find bound states with a small width as can be seen in Figs. 7 and 8. In fact, the widths found are $\sim$5, 4, and 0 MeV for $S = 0$, 1, and 2, respectively.

In Eq. (29), the amplitude close to a pole looks like

$$T_{ij} \approx \frac{g_i g_j}{z - z_R}, \quad (36)$$

where $\mathrm{Re}z_R$ gives the mass of the resonance and $\mathrm{Im}z_R$ the half-width. The constants g_i ($i = \rho D^*$, ωD^*), which provide the coupling of the resonance to one particular chan-

TABLE IV. Pole positions for the three different cases.

I	S	$\sqrt{s}$ (MeV)
1/2	0	2592
1/2	1	2611
1/2	2	2450

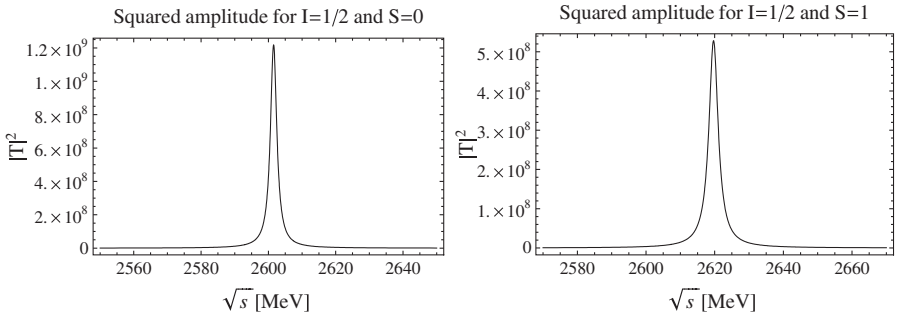

FIG. 7. Squared amplitude for $I = 1/2$ and $S = 0$, 1 including the convolution of the ρ-mass distribution.

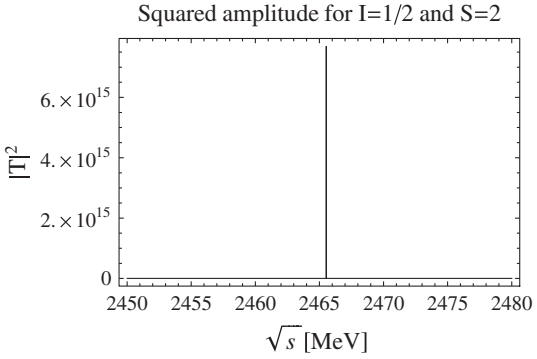

FIG. 8. Squared amplitude for $I = 1/2$ and $S = 2$ including the convolution of the ρ-mass distribution.

nel, can be calculated by means of the residues of the amplitudes as given in Table V. In the PDG [6], two states are listed, $D^*(2640)$ and $D_2^*(2460)$ in the sectors $I(J^P) = 1/2(?^?)$ and $I(J^P) = 1/2(2^+)$, respectively. Comparing with the present model predictions as listed in Table IV, we attempt to identify them with those states of $S = 1$ and $S = 2$, respectively. The reason to identify the $D^*(2640)$ with our pole for the case of $S = 1$ and not $S = 0$ is going to be clear in the next section when the $D\pi$ channel is considered. In the case of the $D^*(2640)$ the width quoted in the PDG is very small, $\Gamma < 15$ MeV. According to our result after taking into account the ρ mass distribution, one obtains 3–4 MeV; see Fig. 7. In the case of $D_2^*(2460)$, the width quoted in the PDG is 43 ± 4 MeV for the D_2^{*0} and 37 ± 6 MeV for $D_2^{*\pm}$. Then, it is clearly not compatible with the width found here, which is zero, see Fig. 8, and we need to allow for the fact that the resonance decays to another channel. For this reason we are going to consider the $D\pi$ channel in the next section, which is below the threshold of ρD^*. A novelty in this work is that we have obtained a new resonance in the sector $I = 1/2$ and $S = 0$ which does not appear in the PDG; see Table IV. One should note that if one takes Eq. (32) instead of Eq. (31) with a cutoff of the order of the natural size $q_{\max} =$ 1–1.2 GeV, the results are very similar to those of Table IV (difference around 1%), which is an indication of the stability of the results.

TABLE V. Modules of the couplings g_i in units of GeV for the poles in the $S = 0$, 1, 2; $I = 1/2$ sector with the channel ρD^* and ωD^*.

Channel	$D_0^*(2600)$	$D_1^*(2640)$	$D_2^*(2460)$
ρD^*	14.32	14.04	17.89
ωD^*	0.53	1.40	2.35

V. UNCERTAINTIES RELATED TO SU(4) BREAKING

All the results in this section have been obtained using Eq. (3) for a g, where for M_V we have taken the mass of the ρ and for f the pion decay constant f_π. Since we have the ρD^* system one could also think of taking

$$g_D = \frac{M_{D^*}}{2f_D}, \tag{37}$$

where $f_D = 160$ MeV. The justification to take g of Eq. (3) is that it is always the ρ meson that is exchanged in the most important terms. However, it is instructive to see what happens when we use g_D instead of g of Eq. (3). In order to estimate uncertainties from this source we will evaluate the results using $g^2 \to g^2$, gg_D, and g_D^2.

In the first step we take gg_D and look at the poles for different states. We make a small readjustment of the substraction constant, α, such as to get the D_2^* state at the same mass as before. The new value is $\alpha = -1.53$, but the masses of the other two states change as one can see in Table VI. In this table we also show the results that we obtain for the option of using g_D^2 readjusting α to get the

TABLE VI. Pole positions and subtraction constant obtained for the three different cases, g^2, gg_D, and g_D^2, when one fixes the mass of the pole with $S = 2$.

Constant & α	$S = 0$	$S = 1$	$S = 2$
g^2 & -1.74	2592	2611	2450
gg_D & -1.53	2571	2587	2450
g_D^2 & -1.39	2551	2565	2450

TABLE VII. Pole positions for the three states using $\alpha = -1.53$ in the different cases g^2, gg_D, and g_D^2.

$\alpha = -1.53$	$D_0(2600)$			$D_1^*(2640)$			$D_2^*(2460)$		
Cases:	g^2	gg_D	g_D^2	g^2	gg_D	g_D^2	g^2	gg_D	g_D^2
$\sqrt{s}$ (MeV)	2645	2571	2502	2661	2587	2517	2539	2450	2370

TABLE VIII. Modules of the couplings g_i in units of GeV for the poles in the $S = 0, 1, 2$; $I = 1/2$ sector and the channels ρD^* and ωD^*, in the cases (1) using g^2 and $\alpha = -1.74$, (2) using gg_D and $\alpha = -1.53$, and (3) using g_D^2 and $\alpha = -1.39$.

Channel	$D_0(2600)$			$D_1^*(2640)$			$D_2^*(2460)$		
Cases:	(1)	(2)	(3)	(1)	(2)	(3)	(1)	(2)	(3)
ρD^*	14.32	15.69	17.05	14.04	15.37	16.69	17.89	19.58	21.01
ωD^*	0.53	0.68	0.84	1.40	1.69	1.99	2.35	2.60	2.78

right mass for the D_2^* state. As we can see, the mass of the spin zero and one resonance moves by about 20 MeV, a moderate change. This is a realistic way of looking at the uncertainties, since the fine-tuning of the parameter α to get the precise position of one resonance is always done.

We can however look at the problem from a more extreme point of view, taking a fixed α for the different options. The results can be seen in Table VII where $\alpha = -1.53$ such that the D_2^* state has the same mass as before for the option of gg_D. We can observe changes in the mass of the resonances of the order of 70–90 MeV. These changes are typical of any hadron model upon reasonable changes of the parameters. Yet, it is interesting to observe what happens to the couplings of the resonances to the different channels, which are shown in Tables VIII and IX. Table VIII corresponds to the case where the couplings are readjusted to get the D_2^* mass right, while Table IX corresponds to the case of fixed α for all the options. We observe in both cases changes of the order of 8% for the couplings to ρD^*, which is the important one, with respect to the middle option of using gg_D. The couplings to the channel to ωD^* experience a larger variation, but this channel plays

TABLE IX. Modules of the couplings g_i in units of GeV for the poles in the $S = 0, 1, 2$; $I = 1/2$ sector and the channels ρD^* and ωD^*.

Channel	$D_0(2600)$			$D_1^*(2640)$			$D_2^*(2460)$		
$\alpha = -1.53$	g^2	gg_D	g_D^2	g^2	gg_D	g_D^2	g^2	gg_D	g_D^2
ρD^*	14.51	15.69	16.32	14.08	15.37	16.06	18.15	19.58	20.67
ωD^*	0.37	0.68	1.12	1.19	1.69	2.28	2.20	2.60	3.03

essentially no role in the problem. Even then, in the preferred case of readjustment of the α parameter to get the D_2^* mass, the changes of these couplings are below 25%, as one can see in Table VIII. Since the couplings of the resonance to the channels are the basic characteristic of the resonance concerning its nature as a VV state, the stability of the magnitude upon breaking of SU(4) symmetry is certainly a most welcome feature. In view of this discussion and the results found, we proceed further to study other issues concerning those states. In what follows we take the g^2 option, but the results of this section have given us an idea of intrinsic uncertainties of the model that one must keep in mind.

VI. THE πD DECAY MODE

A. Evaluation of the πD-box diagram

In the previous section we have obtained the positions of the poles and obtained a small width for the states taking into account the finite width of ρ. Here we consider a dominant decay mode into the πD channel in order to give account of a finite width. Our starting point is the set of diagrams of Fig. 9. One needs the $\rho\pi\pi$ and the $D^*\pi D$ vertices which are provided within the same hidden gauge formalism [1,2], used in Sec. II, by means of the Lagrangian

$$\mathcal{L}_{V\Phi\Phi} = -ig\langle V^\mu[\Phi, \partial_\mu\Phi]\rangle. \tag{38}$$

For the first diagram of Fig. 9 we have

$$-it^{(\pi D)} = \int \frac{d^4q}{(2\pi)^4}(-i)^4 g^4(\sqrt{2})^2\left(\frac{1}{\sqrt{2}}\right)^2 (k_1 - 2q)^\mu \epsilon_\mu^{(1)}(k_3 - 2q)^\nu \epsilon_\nu^{(3)}(P + k_1 - 2q)^\alpha \epsilon_\alpha^{(2)}(P + k_3 - 2q)^\beta \epsilon_\beta^{(4)} \frac{i}{q^2 - m_\pi^2 + i\epsilon} \times \frac{i}{(k_1 - q)^2 - m_\pi^2 + i\epsilon}\frac{i}{(P - q)^2 - m_D^2 + i\epsilon}\frac{i}{(k_3 - q)^2 - m_\pi^2 + i\epsilon}. \tag{39}$$

Using the approximation that all the polarization vectors are spatial, it is possible to write the above amplitude as

$$-it^{(\pi D)} = g^4 \int \frac{d^4q}{(2\pi)^4} 16 q_i q_j q_l q_m \epsilon_i^{(1)}\epsilon_j^{(2)}\epsilon_l^{(3)}\epsilon_m^{(4)} \frac{1}{q^2 - m_\pi^2 + i\epsilon}\frac{1}{(k_1 - q)^2 - m_\pi^2 + i\epsilon}\frac{1}{(P - q)^2 - m_D^2 + i\epsilon} \times \frac{1}{(k_3 - q)^2 - m_\pi^2 + i\epsilon}. \tag{40}$$

This integral is logarithmically divergent and as in [4] we regularize it with a cutoff in the three-momentum of the order of

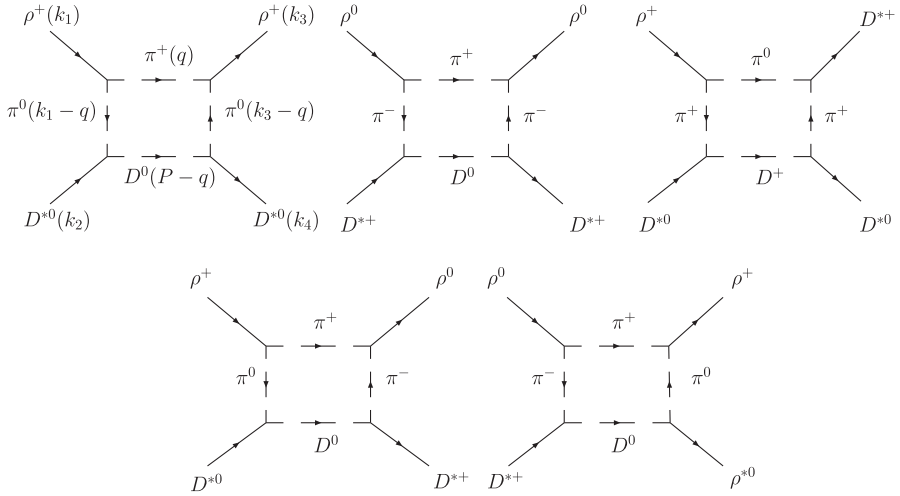

FIG. 9. πD-box diagrams.

the natural size, for which we take $q_{\max} = 1.2$ GeV. The results do not change much if one takes a value around this. After performing the dq^0 integral of Eq. (40), one finds

$$V^{(\pi D)} = g^4(\epsilon_i^{(1)}\epsilon_i^{(2)}\epsilon_j^{(3)}\epsilon_j^{(4)} + \epsilon_i^{(1)}\epsilon_j^{(2)}\epsilon_i^{(3)}\epsilon_j^{(4)} + \epsilon_i^{(1)}\epsilon_j^{(2)}\epsilon_j^{(3)}\epsilon_i^{(4)})\frac{8}{15\pi^2}\int_0^{q_{\max}} dq\vec{q}^6\left(\frac{1}{2\omega}\right)^3\left(\frac{1}{k_1^0+2\omega}\right)^2\frac{1}{k_2^0-\omega-\omega_D+i\epsilon}$$
$$\times\frac{1}{k_4^0-\omega-\omega_D+i\epsilon}\frac{1}{k_1^0-2\omega+i\epsilon}\frac{1}{k_3^0-2\omega+i\epsilon}\frac{1}{P^0-\omega-\omega_D+i\epsilon}\frac{1}{P^0+\omega+\omega_D}$$
$$\times\left(\frac{1}{k_2^0+\omega+\omega_D}\right)^2\frac{1}{2\omega_D}f(P^0), \tag{41}$$

where

$$f(P^0) = 4\{-32k_3^0P^0\omega^2\omega_D((P^0)^2-2\omega^2-3\omega\omega_D-\omega_D^2) + 2(k_3^0)^3P^0\omega_D((P^0)^2-5\omega_D^2-2\omega\omega_D-\omega_D^2)$$
$$+ (k_3^0)^4(2\omega^3-(P^0)^2\omega_D+3\omega^2\omega_D+2\omega\omega_D^2+\omega_D^3) + 4\omega^2(8\omega^5+33\omega^4\omega_D+54\omega^3\omega_D^2+3\omega_D((P^0)^2-\omega_D^2)^2$$
$$+ 18\omega\omega_D^2(-(P^0)^2+\omega_D^2) + \omega^2(-12(P^0)^2\omega_D+44\omega_D^3)) - (k_3^0)^2(16\omega^5+63\omega^4\omega_D+74\omega^3\omega_D^2+\omega_D((P^0)^2$$
$$-\omega_D^2)^2+32\omega^2\omega_D(-(P^0)^2+\omega_D^2)+\omega(-6(P^0)^2\omega_D^2+6\omega_D^4))\}, \tag{42}$$

$\omega = \sqrt{\vec{q}^2+m_\pi^2}$, $\omega_D = \sqrt{\vec{q}^2+m_D^2}$, and $P^0 = k_1^0 + k_2^0$. In Eq. (41) we can see clearly the sources of the imaginary part in the cuts $k_2^0(k_4^0) - \omega - \omega_D = 0$, $k_1^0(k_3^0) - 2\omega = 0$, and $P^0 - \omega - \omega_D = 0$, which give rise to the decays $D^{*0} \to \pi D$, $\rho \to \pi\pi$, and $\rho D^{*0} \to \pi D$, respectively. As in [4], to take into account the ρ mass distribution, we make a simple approach. First we neglect the three-momenta of external particles ($\vec{k}_i \sim 0$, $i = 1, 2, 3, 4$) and approximate $k_1^0 \sim k_3^0 \sim m_\rho$ and $k_2^0 \sim k_4^0 \sim m_{D^*}$. Then we find double poles of $(1/(k_1^0 - 2\omega + i\epsilon))^2$ and $(1/(k_2^0 - \omega - \omega_D + i\epsilon))^2$. These double poles are then removed by replacing

$$\left(\frac{1}{k_1^0-2\omega+i\epsilon}\right)^2 \to \frac{1}{k_1^0-2\omega+i\Gamma_\rho/4}\times\frac{1}{k_1^0-2\omega-i\Gamma_\rho/4}, \tag{43}$$

and so on, considering a finite width for ρ and D^*. Here we set $\Gamma_\rho = 146.2$ MeV and $\Gamma_{D^*} = 2.1$ MeV (the results are identical if we put $\Gamma_{D^*} = 0$ MeV). Once this is done, the other diagrams of Fig. 9 are calculated easily, which takes into account the decay into the πD channel. One must make a projection into a proper isospin and spin. For isospin, only $I = 1/2$ is allowed, while for spin, $S = 0$ and 2 are allowed. Decay into $S = 1$ is forbidden since the parity of the ρD^* system for ρ in the s wave is positive, which forces the πD system to be in $L = 0, 2$. Since the π and D have no spin, the total angular momentum J is equal to L in this case. Therefore, only the 0^+, 2^+ quantum numbers have this decay channel. This provides an explanation on why the $D^*(2640)$ does not have a practical width and the $D_2^*(2460)$ has a bigger width. Finally, we obtain

$$t^{(2\pi,I=1/2,S=0)} = 20\tilde{V}^{(\pi D)}, \qquad t^{(2\pi,I=1/2,S=2)} = 8\tilde{V}^{(\pi D)}, \tag{44}$$

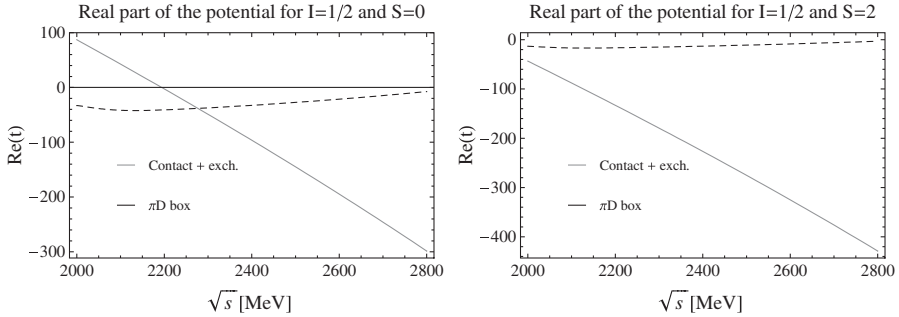

FIG. 10. Real part of the potential for $I = 1/2$; $S = 0$; and $I = 1/2$; $S = 2$.

where $\tilde{V}^{(\pi D)}$ is given by Eq. (41) after removing the polarization vectors. As in [4] we use a form factor for an off-shell π in each vertex, which is

$$F(q) = \frac{\Lambda^2 - m_\pi^2}{\Lambda^2 + \vec{q}^2}, \tag{45}$$

with $\Lambda = 1400$, 1500 MeV. The real and imaginary parts of the potential for the contributions that we have calculated are plotted in Figs. 10 and 11. As we can see, the real part of the potential coming from the πD-box diagram is much smaller than the real part of the potential coming from the contact plus exchange terms.

The relatively small contribution of the real part of the box diagram has allowed us to neglect it in the approach to the vector-vector interaction. A complete formal treatment of the problem would consider a larger set of coupled channels where vector-vector (VV) and pseudoscalar-pseudoscalar (PP) states would be treated on an equal footing. Adding the PP channel requires the $PP \to PP$ potential and the $VV \to PP$ transition potential. The former potential is provided by the exchange of vector mesons and extra contact terms [1–3]. The latter $VV \to PP$ transition has appeared in the box diagram calculation in the present section. An important observation here is that the transition potential turns out to be small due to the momentum dependent (p-wave) nature of the Yukawa-type vertex VPP. Therefore, the full coupled channel calculation including all orders is not necessary in practice and only the lowest contribution is sufficient. For the decay width this corresponds to the calculation of the box diagram. The realization that the $VV \to PP$ transition is relatively small also indicates that the VV and PP systems are largely disentangled in this formalism.

B. Results with $V^{(\pi D)}$

In Fig. 12 we show the results when one introduces the amplitudes of Tables I, II, and III and the given ones in Eqs. (44) and (41) in the Bethe-Salpeter equation (29). As one can see, now the states for $S = 0$ and $S = 2$ have a larger width since they can decay to πD also. We have found a width of 20 MeV for the $D_2^*(2460)$, which is about 50% of the total width quoted in the PDG [6]. One could also have the $D^*\pi$ decay channel, which would be possible by means of an anomalous coupling but, as it was seen in [4], this leads to a smaller contribution than the other one. Also in the PDG the most important contribution comes from the πD channel. For the case of the new state found the width obtained is 50 MeV with $\Lambda = 1500$ MeV. In the next section we introduce new elements of phenomenology that help obtain a somewhat larger width.

C. Results with $V^{(\pi D)}$ using a different form factor and the experimental coupling constant $g_{D^*D\pi}$

In this section we would like to evaluate again the πD-box diagram, but, taking into account the strong coupling $g_{D^*D\pi}$ and a different form factor also for an off-shell pion. After the recent measurements by the CLEO Collaboration [23], it is known that the D^* meson couples

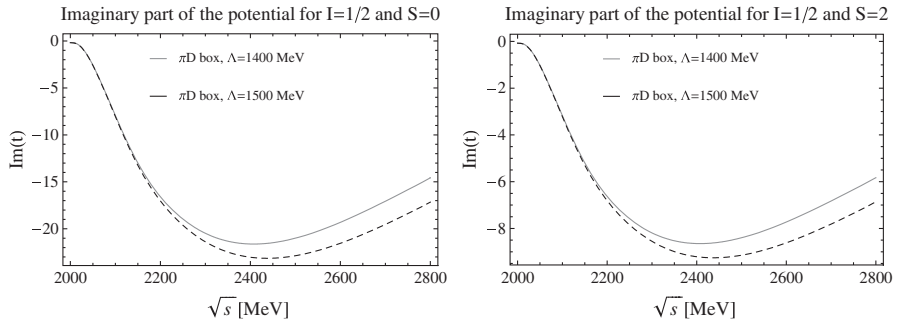

FIG. 11. Imaginary part of the potential for $I = 1/2$; $S = 0$; and $I = 1/2$; $S = 2$.

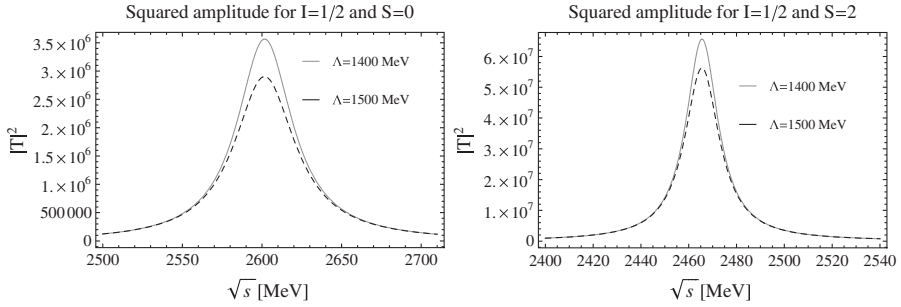

FIG. 12. Squared amplitude for $S = 0$ and $S = 2$ including the convolution of the ρ-mass distribution and the πD-box diagram.

strongly to $D\pi$. The experimental value of this coupling turns out to be larger, almost by a factor of 2, than the value obtained from some of the theoretical predictions using different approaches of the QCD sum rule [24,25]. Within the hidden gauge formalism, the vertex $D^{*+}D^0\pi^-$ obtained from Eq. (38) is

$$\langle D^{*+}(p)\pi^-(q)|D^0(p+q)\rangle = -2g'_{D^*D\pi}q_\mu\epsilon^\mu, \qquad (46)$$

with $g'_{D^*D\pi} = m_{D^*}/2f_D = 6.3$, which is also smaller than the experimental value for this, $g^{\rm exp}_{D^*D\pi} = 8.95 \pm 0.15 \pm 0.95$. In [26], the $D^*D\pi$ form factor is evaluated using the QCD sum rule for a D or a π off shell. A parametrization for an off-shell pion in terms of a form factor

$$F'(q^2) = g_{D^*D\pi}e^{q^2/\Lambda^2}, \quad \text{with} \quad \Lambda = 1.2 \text{ GeV}, \qquad (47)$$

is taken, together with another form factor to account for off-shell D mesons, which we do not need here since we are concerned about the imaginary part of the box diagram where the D meson will be on shell. In Eq. (47) q^2 is a four-momentum square $q^2 = q^{02} - \vec{q}^2$. With these assumptions on the form factors, a value of $g_{D^*D\pi} = 2g'_{D^*D\pi} = 14.9$ is obtained in [26], which would be in better agreement with experiment ($g'_{D^*D\pi} = 7.45$).

For the first diagram of Fig. 9, we consider the q^0 component of the π^+ on shell, hence

$$q_0 = \frac{s + m_\pi^2 - m_D^2}{2\sqrt{s}} \sim 769.4 \text{ MeV}$$

and $(k_1^0 - q^0) \sim 6$ MeV, for ρD^* at threshold, in the approximation of momentum zero for external particles. This leads to $(k^0 - q^0)^2/\Lambda^2 \sim 10^{-5}$, for values of Λ around 1 GeV. Then it is licit to use the three-momentum version of the form factor of Eq. (47) for an off-shell pion in each of the vertices, that is, we replace in Eq. (41) the factor g^4 by

$$g^2_{\rho\pi\pi}(g^{\rm exp}_{D^*D\pi})^2(e^{-\vec{q}^2/\Lambda^2})^4, \qquad (48)$$

with $g_{\rho\pi\pi} = m_\rho/2f_\pi = 4.2$ and $g^{\rm exp}_{D^*D\pi} = 8.95$ MeV (the experimental value), $\Lambda \sim 1$–1.2 GeV and $\vec{q}$ running in the integral.

In Figs. 13 and 14 we show the real and imaginary parts of the potential using Eqs. (41) and (48). As we can see, the real part of the πD-box diagram is very small compared with those coming from the contact term plus vector exchange terms, and therefore we can ignore it, thus focusing our attention at the imaginary part. The imaginary part is now larger than that in Fig. 11, but is still comparable with the values quoted in the PDG [6] for the width. We show the $|T|^2$ in Fig. 15 for various cutoff parameters. The $|T|^2$ is similar to Fig. 12, but now the width is slightly larger. In the case of $\Lambda = 1$ GeV, we obtain 40 MeV for $S = 2$, very close to the value quoted by the PDG (43 ± 4 MeV), and 61 MeV for $S = 0$. For $\Lambda = 1.2$ GeV we obtain for $S = 2$ a width around 60 MeV. Therefore, the two form factors, Eqs. (45) and (48), provide reasonable values of the width, with a preference for the option using the experimental $g^{\rm exp}_{D^*D\pi}$ value and $\Lambda = 1$ GeV in Eq. (48).

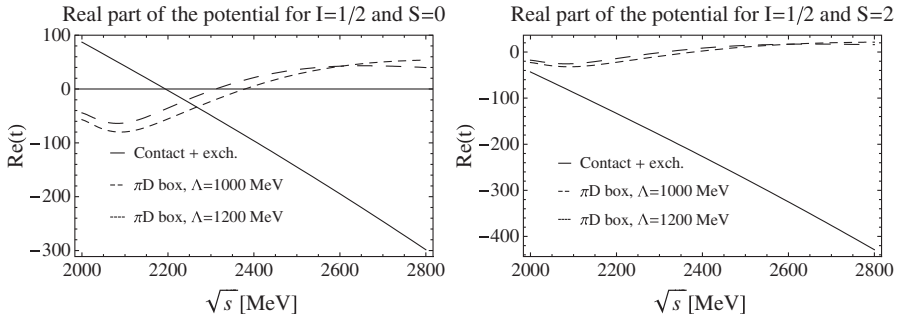

FIG. 13. Real part of the potential for $I = 1/2$; $S = 0$; and $I = 1/2$; $S = 2$.

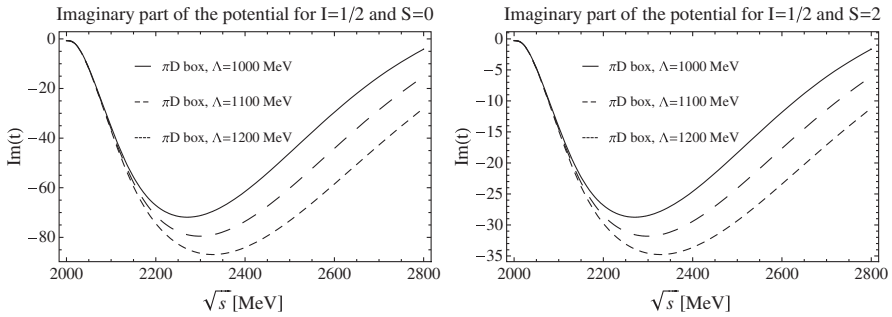

FIG. 14. Imaginary part of the potential for $I = 1/2$; $S = 0$; and $I = 1/2$; $S = 2$.

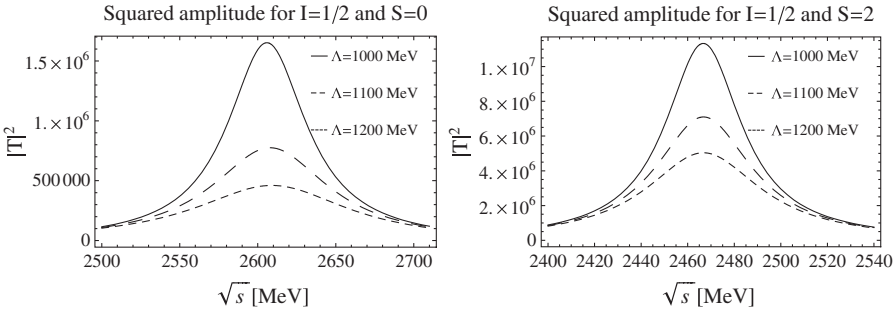

FIG. 15. Squared amplitude for $S = 0$ and $S = 2$ including the convolution of the ρ-mass distribution and the πD-boxed diagram.

VII. CONCLUSIONS

We have made a study of the $(\rho\omega)D^*$ interaction using the hidden gauge formalism. The interaction comes from contact terms plus ρ meson exchange in the t channel. Of all spin and isospin allowed channels in the s wave, we found strong attraction, enough to bind the system, in $I = 1/2$, $S = 0$, $I = 1/2$, $S = 1$, and $I = 1/2$, $S = 2$. We also found that in the case of $I = 1/2$, $S = 2$ the interaction was more attractive than in the other two cases, leading to a tensor state more bound than the scalar and the axial vector. The consideration of the ρ mass distribution gives a width to the three states, rather small in all cases. Consideration of the πD decay channel, in an equivalent way to what was done in the case of the $\rho\rho$ interaction going to $\pi\pi$ in [4], makes the widths larger and realistic. Yet, the smaller phase space available here makes this contribution relatively smaller than in the case of the $\rho\rho$ interaction. We found that the tensor state obtained matches the properties of the tensor state $D_2^*(2460)$. We predict two more states with $S = 0$ and $S = 1$, which are less bound than the tensor state. We find in the PDG the state $D^*(2640)$ without experimental spin and parity assigned, but we conjecture that this state should be the $S = 1$ state found by us because we could find a natural explanation for the small experimental width of this state. The other state nearly degenerate in energy with this one, but with spin $S = 0$, is yet to be found. The results obtained here should stimulate the search for more D states in the region of 2600 MeV.

ACKNOWLEDGMENTS

This work is partly supported by DGICYT Contract No. FIS2006-03438. We acknowledge the support of the European Community-Research Infrastructure Integrating Activity Study of Strongly Interacting Matter (acronym HadronPhysics2, Grant Agreement No. 227431) under the Seventh Framework Programme of EU. A. H. is supported in part by the Grant for Scientific Research Contract No. 19540297 from the Ministry of Education, Culture, Science and Technology, Japan. H. N. is supported by the Grant for Scientific Research No. 18-8661 from JSPS.

[1] M. Bando, T. Kugo, S. Uehara, K. Yamawaki, and T. Yanagida, Phys. Rev. Lett. **54**, 1215 (1985).
[2] M. Bando, T. Kugo, and K. Yamawaki, Phys. Rep. **164**, 217 (1988).
[3] M. Harada and K. Yamawaki, Phys. Rep. **381**, 1 (2003).
[4] R. Molina, D. Nicmorus, and E. Oset, Phys. Rev. D **78**,

114018 (2008).
[5] H. Nagahiro, J. Yamagata-Sekihara, E. Oset, S. Hirenzaki, and R. Molina, Phys. Rev. D **79**, 114023 (2009).
[6] C. Amsler *et al.* (Particle Data Group), Phys. Lett. B **667**, 1 (2008).
[7] S. Uehara (private communication).
[8] L. S. Geng and E. Oset, Phys. Rev. D **79**, 074009 (2009).
[9] C. Garcia-Recio, V. K. Magas, T. Mizutani, J. Nieves, A. Ramos, L. L. Salcedo, and L. Tolos, Phys. Rev. D **79**, 054004 (2009).
[10] L. S. Geng and J. Nieves (unpublished).
[11] J. Nieves (private communication).
[12] S. Godfrey and N. Isgur, Phys. Rev. D **32**, 189 (1985).
[13] F. E. Close and E. S. Swanson, Phys. Rev. D **72**, 094004 (2005).
[14] H. Nagahiro, L. Roca, A. Hosaka, and E. Oset, Phys. Rev. D **79**, 014015 (2009).
[15] Riazuddin and Fayyazuddin, Phys. Rev. **147**, 1071 (1966).
[16] J. J. Sakurai, *Currents and Mesons* (University of Chicago Press, Chicago, IL, 1969).
[17] J. Gasser and H. Leutwyler, Nucl. Phys. **B250**, 465 (1985).
[18] U. G. Meissner, Rep. Prog. Phys. **56**, 903 (1993).
[19] T. Hyodo, D. Jido, and A. Hosaka, Phys. Rev. D **75**, 034002 (2007).
[20] T. Hyodo, D. Jido, and A. Hosaka, Phys. Rev. Lett. **97**, 192002 (2006).
[21] J. A. Oller and E. Oset, Phys. Rev. D **60**, 074023 (1999).
[22] J. A. Oller and U. G. Meissner, Phys. Lett. B **500**, 263 (2001).
[23] S. Ahmed *et al.* (CLEO Collaboration), Phys. Rev. Lett. **87**, 251801 (2001).
[24] V. M. Belyaev, V. M. Braun, A. Khodjamirian, and R. Ruckl, Phys. Rev. D **51**, 6177 (1995).
[25] P. Colangelo, G. Nardulli, A. Deandrea, N. Di Bartolomeo, R. Gatto, and F. Feruglio, Phys. Lett. B **339**, 151 (1994).
[26] F. S. Navarra, M. Nielsen, and M. E. Bracco, Phys. Rev. D **65**, 037502 (2002).